Use of Constrained G-Quadruplexes for Enantioselective Sulfoxidation Site Mapping

Yoann Colas, Stéphane Ménage, Caroline Marchi- Delapierre, Nicolas Spinelli

USE OF CONSTRAINED G-QUADRUPLEXES FOR ENANTIOSELECTIVE SULFOXIDATION SITE MAPPING

Dr. Yoann Colas,[a],[b] Dr. Stéphane Ménage,[a] Dr. Caroline Marchi-Delapierre,[a] Prof. Nicolas Spinelli[b],*

[a] Univ Grenoble Alpes, CNRS, CEA,
Laboratoire de Chimie et Biologie des Métaux,
17 Avenue des martyrs,
38000 Grenoble, France

[b] Univ. Grenoble-Alpes
Département de Chimie Moléculaire
UMR CNRS 5250
CS 40700
38058 Grenoble, France

E-mail: Nicolas.Spinelli@univ-grenoble-alpes.fr

Homepage: https://dcm.univ-grenoble-alpes.fr/membre/nicolas-spinelli

Supporting information for this article is given via a link at the end of the document

Abstract: Catalysis using G-quadruplexes (G-4) has shown promise as a way to perform asymmetric sulfoxidation of thioanisole derivatives. However, despite the relative simplicity of G-4, the mechanism of chiral control of sulfoxidation is still unknown, mainly because G-4 can adopt different topologies. To better understand the mechanism of G-4-catalyzed sulfoxidation, we chemically constrained G-4 into a unique topology. We show that either sulfoxidation can occur at the outer tetrads or at the grooves of G-4 and that different enantiomers can be generated depending on the region where catalysis occurs. Thus, thanks to our G-4 mimics, we can unravel the enantioselective control of the sulfoxidation reaction.

Introduction

The development of new enantioselective catalysts remains an exciting challenge, especially for the preparation of pharmaceuticals.[1] In this field, biocatalysts, *i.e.*, natural or engineered enzymes, play a key role[2] because they exhibit remarkable enantio- and region-selectivities as well as environmentally friendly experimental conditions. They are often based on the incorporation of a metal cofactor (natural or artificial), which controls the reaction mode, into a protein scaffold that plays the role of a chiral inducer.[3,4] Nevertheless, their use is often limited to natural substrates. It has been proposed to replace the protein moiety with a nucleic acid, and it has been shown that enantioselective transformations (Diels-Alder, Friedel & Crafts, Michael additions, etc.) can be performed.[5–13] In these transformations, stereoselectivity was ensured by the secondary structure of the nucleic acids used (*e.g.* double helix).

G-quadruplexes (G-4), secondary structures that can be adopted by guanine-rich nucleic acids, have previously attracted interest for catalytic purposes, particularly oxidation reactions for diagnostic purposes.[14,15] Indeed, it was shown that the hybrid formed with a G-4 and the natural peroxidase cofactor hemin (iron(III) chloroprotoporphyrin IX), with the porphyrin group stacked on top of apical quartets, was able to mimic the natural peroxidase upon addition of H_2O_2.[16–18] It was also found that this combination could catalyze oxygen transfer reactions but without any enantioselectivity[19] (whereas it is able to catalyze asymmetric cyclopropanation reactions[20,21]).

Replacement of the hemin cofactor by other metal complexes, such as the 4,4'-dimethyl-2,2'-bipyridine copper, Cu(dmbipy), enables G-4-induced enantioselective transformations[22–28] and particularly sulfoxidations.[29,30] Such oxygen transfer reactions play a key role in the synthesis of active pharmaceutical drugs or intermediates.[31] An interesting feature is that the efficiency and enantiomeric excess (*e.e.*) depend on the major topology adopted by the G-4. Some G-4 are indeed capable of adopting different topologies (parallel, antiparallel, and hybrid)[32–35] and for some of these conformations are in equilibrium.[36] This equilibrium can be shifted toward one topology by changing the composition of the buffer (especially cations).[37]

For example, Can Li's group has shown that in the enantioselective sulfoxidation of thioanisole with a 21-mer human telomeric sequence (HT21, d($^{5'}$($G_3T_2A)_3G_3^{3'}$)),[29] a complete conversion is achieved with an *e.e.* of 56 %, in the presence of potassium cations whereas conversion decreases dramatically and enantioselectivity is lost when potassium cations are replaced by sodium ones. Indeed, in the presence of potassium, HT21 adopts a mixture of conformations (parallel, antiparallel, and hybrid, Figure 1, A), whereas in the presence of sodium, it adopts only a less efficient antiparallel conformation. Replacing the DNA sequence with its RNA analog (*e.g.*, $^{5'}$($g_3$uua)$_3g_3^{3'}$), which adopts only the parallel conformation, resulted in a loss of enantioselectivity with a lower conversion of 70 %, meaning that high *e.e.* and efficiency are devoted to the presence of the hybrid conformation. The change in flanking nucleosides and sequences also demonstrates the high sensitivity of this reaction to conformations. In addition, interaction studies have been performed to

determine the site of reaction at HT21.[38] Indeed, interactions of G-4 with organic molecules can occur at either the loops, the grooves, or the external tetrads.[39] The interaction of the Cu(dmbipy) complex with G-4 is modest (K_D above µM) and occurs nonspecifically throughout all the sites. Interaction with thioanisole occurs mainly at the 3' end and the second loop (L2, **Figure 1**, A) of HT21, independent of its topology and with a modest K_D (above 1 µM). However, these interactions do not indicate that enantioselective conversion occurs only at these sites. Taken together, all these results indicate that despite the chemical simplicity of G-4 compared to proteins, the mechanism of enantioselective sulfoxidation by G-4 depends relatively strongly on the topology, the interaction sites of the substrate and, to a lesser extent, the copper complex. These interaction sites can be diverse, and not all are responsible for enantioselective conversion.

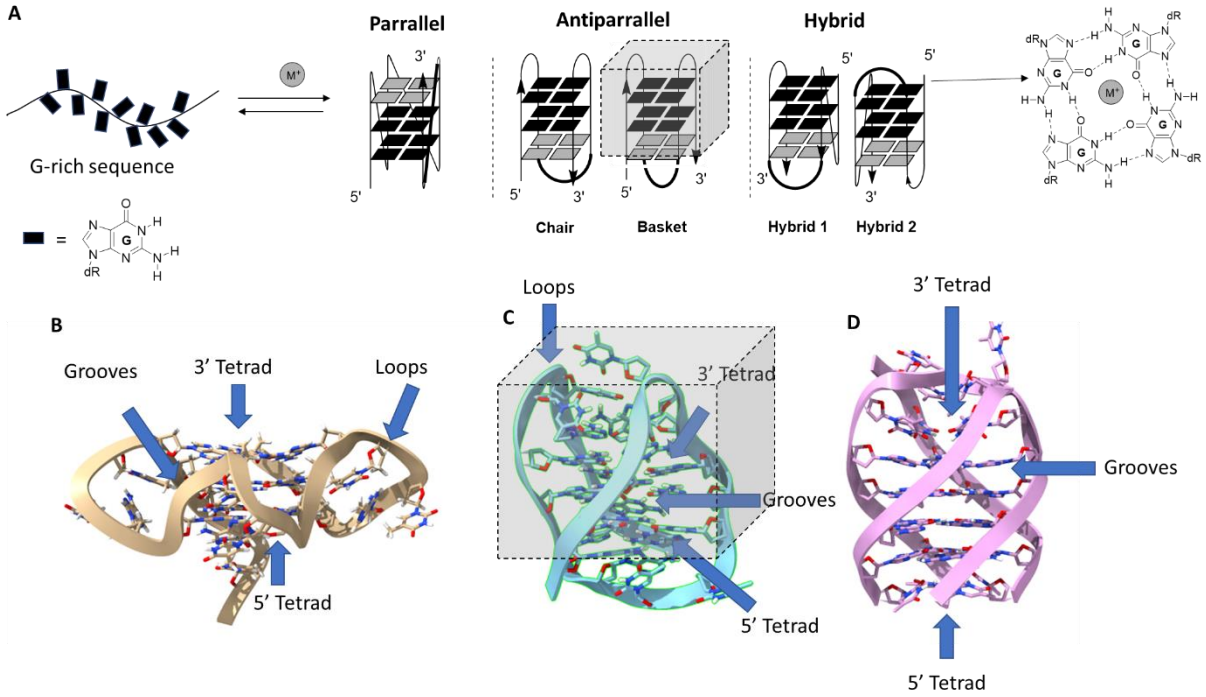

Figure 1. (A) Topological equilibrium for G-4. Putative sites of interaction of thioanisole are highlighted : the 3' tetrad in grey and the L2 loop in bold.[38] 3D Grey cube indicates the part of the G-4 which is mimicked by **2** (vide infra). (B) Three-dimensional structure of the unimolecular parallel G-4 d($^{5'}$TAG$_3$T TAG$_3$T TAG$_3$T TAG$_3^{3'}$) (pdb: 2ld8).[40] (C) Three-dimensional structure of the unimolecular basket type antiparallel G-4 d($^{5'}$AG$_3$T TAG$_3$T TAG$_3$T TAG$_3^{3'}$) (pdb: 143D).[41] The dotted rectangle indicates the part of the G-4 which is mimicked by **2** (vide infra). (D) Three-dimensional structure of the tetramolecular parallel quadruplex [d($^{5'}$TTA G$_3$A$^{3'}$)]4 (pdb : 1NP9).[42]

To achieve a higher correlation between topologies and *e.e.*, we propose to perform enantioselective sulfoxidation of thioanisole derivatives with G-4 constrained in a unique topology. Indeed, we have shown that immobilization of a G-4-forming sequence on a peptide scaffold (RAFT: regioselectively addressable functionalized template) using chemoselective reactions (*e.g.* oxime ether and/or CuAAC, Scheme 1) yields stable G-4 mimics and prevents conversion from one topology to another. Based on this concept, we have developed two series of mimics of the human telomeric sequence, one parallel and one antiparallel (Figure 2).[43,44] For the study of the catalytic mechanism, these mimics provide major advantages over the native G-4. Their structurally stable nature, coupled with the absence of topological changes, facilitates the analysis and comprehension of the underlying phenomena. This stability simplifies the overall structure dissection, which comprises loops, grooves, and tetrads. Indeed, the parallel mimics **1a-h** consist of 3 G tetrads, 4 grooves but no structured loops (only flanking nucleosides). Moreover, compared to the native tetramolecular G-4 (Figure 1, D), only the outer 3'-tetrade (at the opposite of the RAFT) is accessible. Consequently, this type of mimic can be used to elucidate the role of the 3' extremity in catalysis. The antiparallel constrained G-4 **2** mimics the side opposite to that with which the thioanisole interacts most strongly, as shown in the study by Can Li (Figure 1, A and C, dotted rectangles).

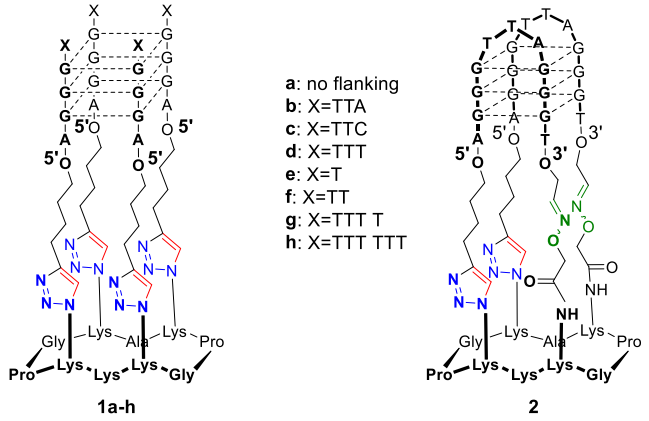

Figure 2. G-4 mimics used in this study. **1a-h** are mimics of the parallel topology of the HT21; **2** of the antiparallel one.

In the present work, we have used these G-4 mimics as chiral scaffolds for the enantioselective sulfoxidation of thioanisole derivatives (Scheme 2), and the results obtained help to decipher the enantioselective control for this transformation, adding to the importance on catalysis of the nature of additional nucleosides over the 3'-tetrad.

Results and Discussion

MIMICS SYNTHESIS AND THEIR CHARACTERISTICS

The G-4 mimics **1a-h** carrying various additional nucleosides at their 3'-end were synthesized using CuAAC by adapting published protocols,[43,44] *i.e.,* by linking 5'-alkyne-modified oligonucleotides **3a-h** to a cyclodecapeptide **4** carrying four azidonorleucines **4** (Scheme 1).

The antiparallel mimic **2** was synthesized by published procedures, *i.e.*, by linking oligonucleotide **5** bearing a 3'-aldehyde and a 5'-alkyne in two steps (oxime ether formation followed by CuAAC) to a RAFT bearing two oxyamino groups and two azidonorleucines **6** (Scheme 1).[44]

All conjugates were purified by RP-HPLC and characterized by UPLC-MS (see supporting information).

The structuring of conjugates **1a-h** was demonstrated by circular dichroism,[45,46] and CD spectra were compared with those of the corresponding native tetrameric oligonucleotides (Figure 3).

In the presence of potassium cations, which favor parallel structuring of G-4 for this sequence,[47,48] the native tetramolecular parallel G-4 and all **1a-h** mimics showed a CD signature characteristic of a parallel G-4 (*i.e.* a minimum around 240 nm and a maximum around 260 nm) (for other mimics and tetramolecular G-4, see supporting information). In the presence of Na^+ or Li^+, which do not favor the formation of a parallel G-4, only the mimics are structured into a parallel G-4 but the native tetramolecular G-4 is not structured. Thus, the scaffold helps stabilizing the chosen topology of the G-4.

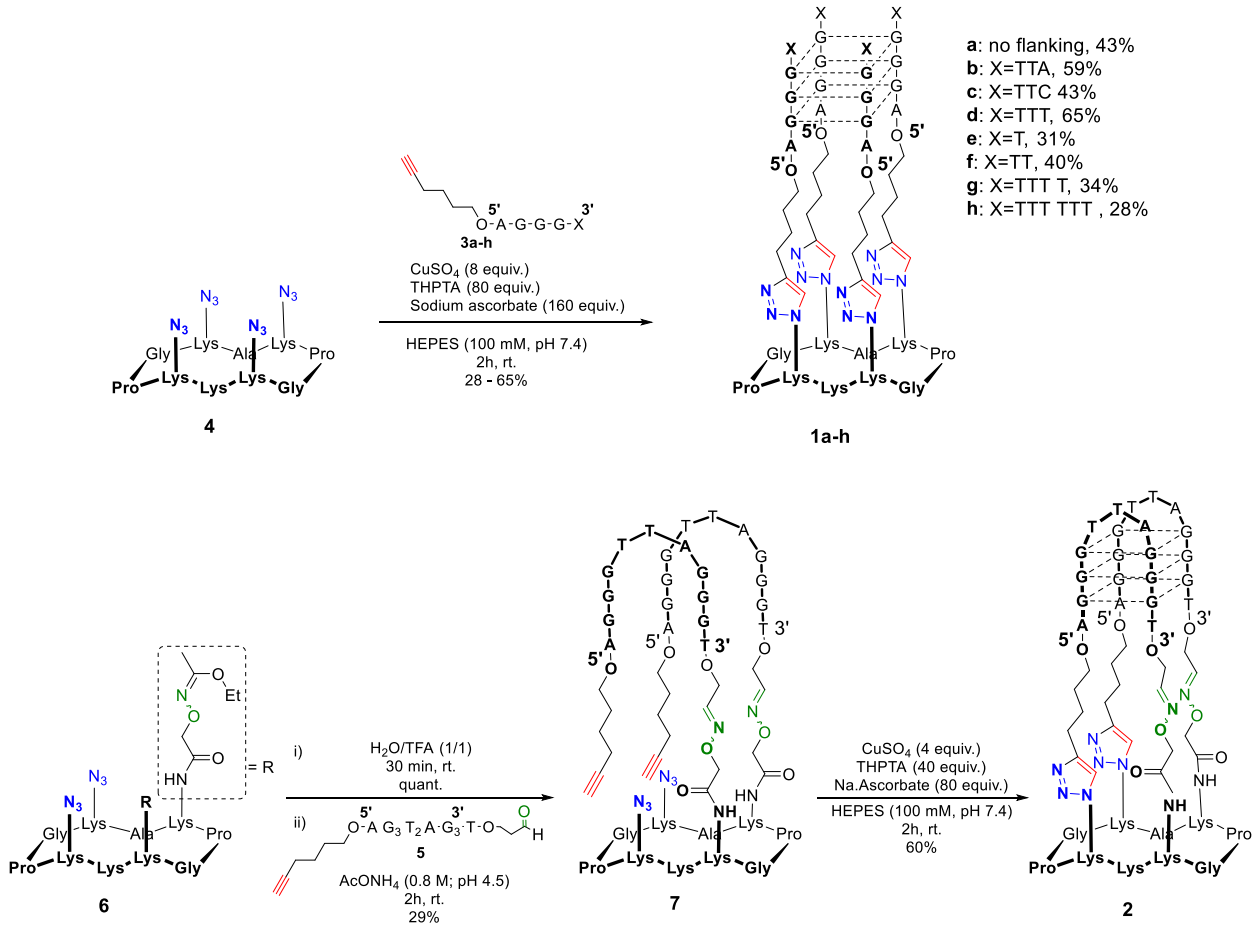

Scheme 1. Synthesis of G-4 mimics **1a-h** and **2**.

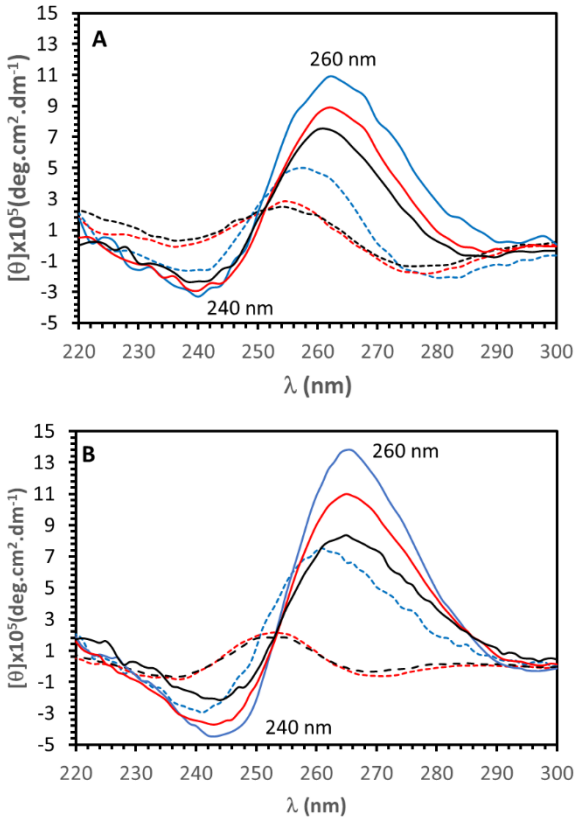

Figure 3. CD spectra recorded at 15°C for: (A) tetramolecular (d($^{5'}$AGG G$^{3'}$), dotted lines); mimic **1a** (plain lines); (B) tetramolecular (d($^{5'}$AGG GTT T$^{3'}$), dotted lines); mimic **1d** (plain lines). CD were performed in the condition of catalysis (MOPS buffer 20 mM, pH 7.0; XCl 150 mM, [1a] = 10 µM; [d(5'AGGG3')] = 40 µM). Blue: X = K^+; red: X = Na^+ and black: X = Li^+.

SULFOXIDATION WITH NATIVE G-4

Catalytic sulfoxidations of *p*-methylthioanisole and 2-bromothioanisole were carried out on 100 µL samples under the same conditions as described previously (Scheme 2; G-4 = d($^{5'}$(G$_3$T$_2$A)$_3$G$_3$)$^{3'}$); XCl = KCl). Yields and *e.e.* were determined by chiral chromatography analyses after extraction with ethyl acetate. Yields were evaluated using calibration curves. *e.e.* were calculated according to formula (1).

$$e.e. = \frac{A_{e2} - A_{e1}}{A_{e1} + A_{e2}} \quad (1)$$

Where A_{e1} and A_{e2} are the area under the chromatographic peak of the first and second eluted enantiomers, respectively.
Using HT21 as a reference, *p*-methylthioanisole and 2-bromothioanisole sulfoxidation yields of 45 and 12 %, respectively, were obtained with *e.e.* of 21 % and -46 %, respectively. The enantiomeric excess obtained for *p*-methylthioanisole was comparable to that previously described (22 % *vs* 29 %)[29] validating our protocol. The absolute configurations of the eluted enantiomers were not determined.
We were able to investigate the influence of the proportion of HT21 on the reaction. For this purpose, Cu(dmbipy) was kept at 1 mol % substrate, and the HT21/Cu(dmbipy) ratio was increased from 0.2 to 2 (Table 1).
Oxidation of *p*-methylthioanisole can take place even without HT21, but without any control of enantioselectivity. At an HT21/substrate ratio of 0.2, moderate *e.e.* is observed with comparable yields. Increasing the HT21/substrate ratio resulted in lower yields but better *e.e.* This trend is the result of competition between rapid oxidation, which occurs without G-4/Cu(dmbipy) interaction and leads to racemic mixtures, and oxidation with G-4/Cu(dmbipy), which provides an asymmetric induction. The observed trend could indicate a saturation behavior of the kinetics due to the binding of substrate or Cudmbipy to the G-4 structure.
Oxidation of 2-bromothioanisole leads to lower yields and racemic mixtures in the absence of HT21. However, when the HT21/substrate ratio is 0.2, an *e.e.* is observed with slightly better yields. Increasing the HT21 ratio does not improve the yield but leads to the same trend of asymmetric induction as with the previous substrate.

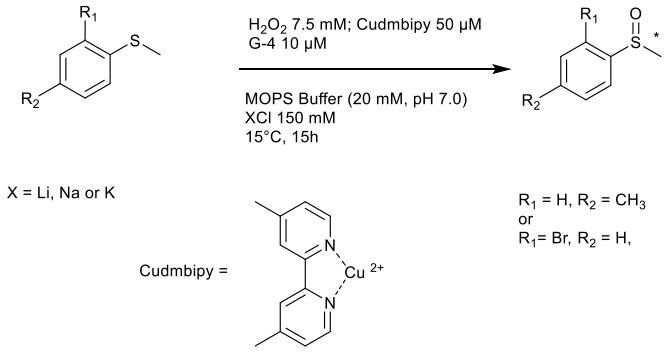

Scheme 2. Sulfoxidation of thioanisole derivatives. G-4 = HT21, tetramolecular G-4, mimic **1a-h** or **2.**

We then investigated the reaction using tetramolecular parallel models of G-4 formed by d($^{5'}$AGG G$^{3'}$). While the oxidation of p-methylthioanisole appears to occur with a slightly better yield when the ratio [d($^{5'}$AGG G$^{3'}$)]$_4$/Cu(dmbipy) is 0.2, the addition of more G-4 is detrimental to the yield. Moreover, no enantioselectivity is observed with this G-4. Thus, we conclude that *p*-methylthioanisole is not a suitable model substrate since the reaction mainly occurs outside the parallel G-4. Therefore, we focused our efforts on 2-bromothioanisole.

Surprisingly, substitution of HT21 with [d($^{5'}$AGG G$^{3'}$)]$_4$ for 2-bromothioanisole did not improve the yield but resulted in a lower and opposite *e.e.* This result was unexpected because no asymmetric induction was observed with a unimolecular parallel RNA G-4.[29] This can be explained by the fact that the native tetramolecular G-4 has more accessible sites for interaction with substrates (*i.e.*, 3'- and 5'-tetrads and grooves) than a unimolecular one (Figure 1, B and D).

The best ratio is HT21/Cu(dmbipy) of one for 1 % molar Cu(dmbipy) *versus* substrate, confirming the previous study's results.[29]

Table 1. Influence of G-4/Cu(dmbipy) ratio on yields and *e.e.* for sulfoxidation of *p*-methylthioanisole and 2-bromothioanisole. G-4 is either HT21 or the native tetramolecular G-4 d($^{5'}$AGG G$^{3'}$)]$_4$ [a], [b],[c]

		p-methylthioanisole		2-bromothioanisole	
G-4	G-4 /Cu(dmbipy)	Yield %	e.e. %	Yield %	e.e. %
none	0	43	0	7	0
HT21	0.2	45	21	12	-46
	1	28	39	13	-62
	2	23	39	12	-64
d($^{5'}$AG GG$^{3'}$)$_4$	0.2	59	0	8	7
	1	43	0	9	9
	2	34	0	9	0

[a] relative errors below 20 % on yields and *e.e.* were determined by statistical comparison of at least 5 experiments. [b] Conditions: [thioanisole derivative] = 5 mM, [Cu(dmbipy)] = 50 µM, [H_2O_2] = 7.5 mM, MOPS buffer 20 mM, [KCl] = 150 mM, 15°C, 5 h. [c] [HT21] varying from 10 to 100 µM, [d($^{5'}$AGG G$^{3'}$)] from 40 to 400 µM (consequently [G-4] from 10 to 100 µM).

SULFOXIDATION WITH PARALLEL MIMICS

Based on the above results, we used 2-bromothioanisole as the substrate with a G-4/Cu(dmbipy) ratio of one to compare the catalytic efficiencies of mimics **1a-h** to those of the equivalent native tetramolecular G-4 (Figure 4).

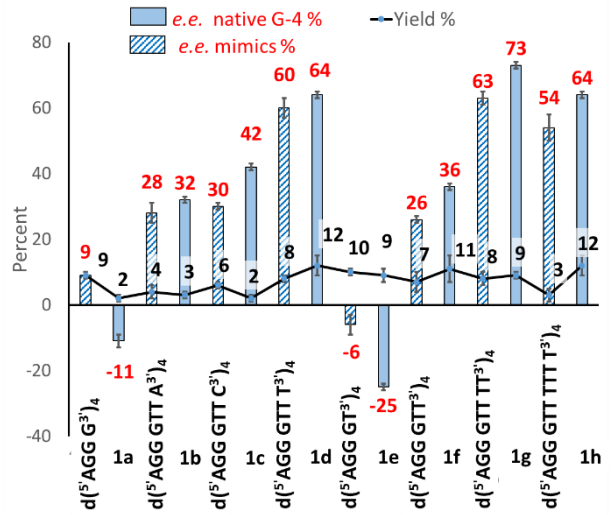

Figure 4. Yields and *e.e.* obtained for the catalytic sulfoxidation of 2-bromothianisole with 1 % Cu(dmbipy), in presence of parallel tetramolecular G-4 (dashed bars) or of mimics **1a-h** (plains bars).

Despite the low observed yields, *e.e.* were determined and tendencies could be identified. First, for native tetramolecular G-4, *e.e.* were almost all positive, indicating that one enantiomer was mostly produced throughout the reaction.

When the reaction was carried out with mimic **1a**, the other enantiomer predominated, as the negative *e.e.* implies.

Considering that no asymmetric reaction was observed with RAFT alone (see supporting information), this suggests that the asymmetric reaction occurs under the influence of the G-4 and that the nature of the peptide drives the location where it occurs, most likely due to the steric hindrance. Assuming that the three interaction sites are available for native tetramolecular G-4 [d($^{5'}$AGG G$^{3'}$)]$_4$ (Figure 1., D), and that the 5'-tetrad is hindered by the RAFT for the corresponding mimic **1a**, the inversion in enantioselectivity can be attributed to differences in reactivity between the three sites. As a result, the *e.e.* obtained with native tetramolecular G-4 was the sum of those obtained for reactions at the two external tetrads and grooves, whereas the *e.e.* obtained with **1a** was the sum of those obtained for reactions at the 3'-tetrad and grooves.

As it has been shown that for unimolecular G-4 (*i.e.*, G-4 with hindered grooves, Figure 1, B), reaction occurs mostly at the 3' extremity,[38] we can deduce that the rates of reactions at the three sites differ.

The effect of introducing three extra nucleosides at the 3' extremity was then investigated. Catalytic competencies of tetramolecular G-4 d($^{5'}$AGG GTT A$^{3'}$)]$_4$, d($^{5'}$AGG GTT C$^{3'}$)]$_4$, d($^{5'}$AGG GTT T$^{3'}$)]$_4$ and their corresponding mimics **1b**, **1c**, and **1d** were assessed. All yields were maintained and *e.e.* were improved (Figure 4). Furthermore, the identical enantiomer was obtained with tetramolecular G-4 and mimics, indicating that the reaction occurred at the same location of the G-4 in this case. The addition of pyrimidine nucleosides at the 3' extremity appears to be beneficial to asymmetric induction. For instance, *e.e.* of respectively 30 and 42 % were obtained for [d($^{5'}$AGG GTT C$^{3'}$)]$_4$ and its corresponding mimic **1c**, while *e.e.* of 60 % and 64 % were obtained for [d($^{5'}$AGG GTT T$^{3'}$)]$_4$ and **1d**.

Under standard conditions, no effect of the cyclodecapeptide alone on catalysis was observed. The addition of three nucleosides at each 3' extremity was hypothesized to interfere with the reaction due to steric hindrance. As a result, the reaction occurs mostly at the 5' extremity and the grooves for tetramolecular G-4 and solely at the grooves for mimics. When the reaction occurs at the 3' extremity, one enantiomer is obtained (the one that is eluted at the first position, providing negative *e.e. cf.* formula 1), while the other is obtained when the reaction occurs at the 5' extremity and the grooves. Furthermore, extra nucleosides appear to boost reaction in the grooves, as *e.e.* for **1b**, **1c**, and **1d** were increased. The higher value of *e.e.* obtained with TTC (**1c**) and TTT (**1d**) suggests that pyrimidine nucleosides improve these interactions.

Therefore, we focused on the impact of adding 1 to 6 thymidines at the 3' extremity (Figure 4). Adding just one thymidine results in a negative *e.e.* for both tetramolecular G-4 and mimic **1e**, suggesting that the reaction occurs at the 3' extremity and that the extra thymidines improve interaction with the substrate.

Then, adding two to six thymidines generates the other enantiomer with increasing efficiency, with a plateau at four thymidines. To further investigating the effect of nucleoside addition on G-4, thermal denaturation measurements were conducted under the same conditions as for the catalytic reaction (MOPS buffer 20 mM, pH 7.0; KCl 150 mM). The melting temperature (Tm, determined by CD) of the tetramolecular G-4 formed by the sequence d($^{5'}$AGG GTT T$^{3'}$) was 53 °C, whereas Tm of the G-4 formed by d($^{5'}$AGG GTT TTT T $^{3'}$) was 41 °C, indicating structural destabilization due to the addition of thymidines. Furthermore, the melting temperatures of the corresponding mimics **1d** and **1h** were over 90°C, suggesting a considerable increase in stability for constrained G-4 structures. These

findings indicate that the higher *e.e.* observed with the mimics is due to both the steric hindrance of the 5' tetrad and the enhanced stability of the parallel G-4 conformation.

To clarify the influence of thymidines, catalytic experiments were performed with nonstructured polythymidines (dT_{21} and dT_7 instead of G-4). Surprisingly, *e.e.* of -25 % and -22 % were observed with yields of 7 % and 8 %, respectively, indicating a predominance of one enantiomer, but not the same as that obtained with structured G-4. These results may indicate that the reaction performed with thymidine-modified G-4 does not occur only at the thymidine tail, but either at structured thymidines (thanks to the G-4) or at the G-4 with the help of the added thymidines. We performed Tm measurements, showing that no stabilization of G-4 occurs when thymidines are added to mimics, suggesting that these nucleosides are not structured (*e.g.*, by the formation of T-tetrads).[49] Indeed, the Tm of **1e, 1d**, and **1h** (MOPS buffer 20 mM, pH 7.0; LiCl 150 mM) were 59 °C, 37 °C, and 33 °C, respectively.

All of these findings lead us to suggest the following model of enantioselective control for tetramolecular G-4, whether native or mimic (Figure 5).

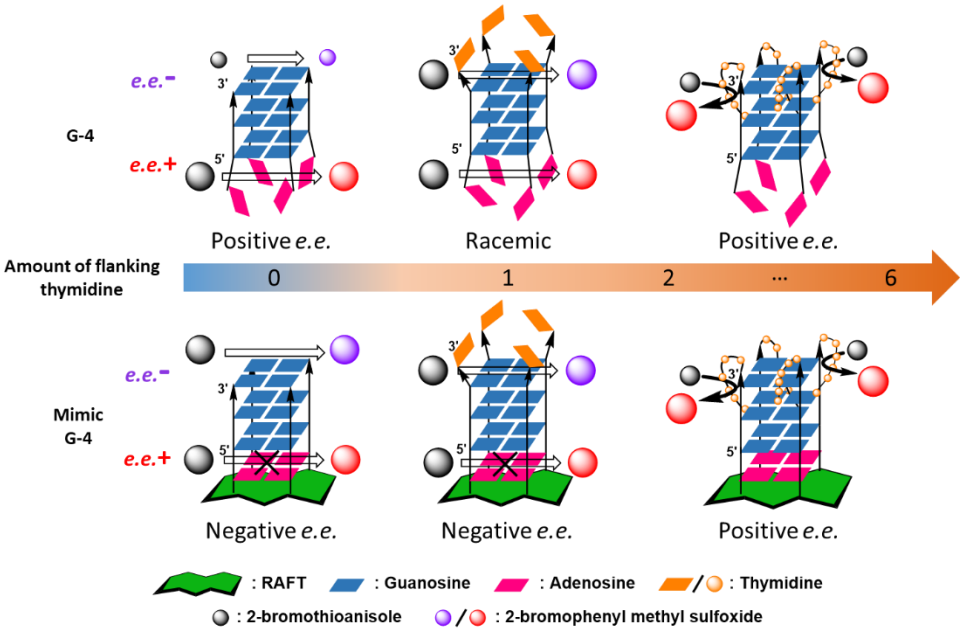

Figure 5. the three-site hypothesis. On the top left structure, the sphere representing 2-bromothioanisole and 2-bromophenyl methyl sulfoxide are smaller than the other ones because of a lower rate of reaction.

Sulfoxidation can occur at the 3'-tetrad, 5'-tetrad, or grooves. The *e.e.* value is determined by the balance of opposing reactions that give one enantiomer when occurring at the 3' tetrad and the other when occurring at the 5'-tetrad or grooves.

In the absence of extra nucleosides (Figure 5, first column), the reaction can occur at both tetrads and grooves. However, because of the presence of additional adenosines at the 5'-tetrad, the reaction is favored there compared to the bared 3' tetrad. The RAFT inhibits access to the 5'-tetrad, causing the reaction to occur solely at the 3'-tetrad and marginally at the grooves. When one thymidine is added at the 3'-tetrad (Figure 5, second column), the probability of the reaction increases at this position, but it results in the opposite enantiomer of the one formed at the 5'- tetrad. Indeed, the nucleosides closest to the external guanine tetrads (A at the 5'-end and T at the 3'-end) may interact with the copper complex, the substrate, or both, facilitating the reaction.[50,51] For tetrameric G-4 alone, this results in a racemic mixture and a negative *e.e.* for the corresponding mimic. Finally, we hypothesize that, like asymmetric induction in double-stranded DNA, which has been demonstrated to occur in grooves,[52,53] asymmetric induction in G-4 grooves can occur. As a result, when more nucleosides are added at the 3'-tetrad (Figure 5, third column), they can overlap the grooves and offer additional interaction with the copper complex, the substrate, or both, so enhancing the reaction. The availability of four reactive sites in the case of a reaction in the grooves (compared to only one for each tetrad) explains the greater absolute *e.e.* found for these G-4 compared to those with fewer nucleosides at the 3'-tetrad.

Then we took advantage of the mimics' stability. Indeed, their structure is less affected by the medium. To demonstrate this point, sulfoxidation was carried out with either the tetramolecular d($^{5'}$AGG GTT T$^{3'}$)$_4$ or its mimic **1d** with various counterions (Li^+, Na^+, or K^+, Table 2).

Catalysis with native G-4 is extremely sensitive to the counterion nature, as evidenced by a decrease in absolute value of *e.e.* when potassium is replaced by sodium or lithium; in fact, tetramolecular parallel G-4 is only formed in the presence of potassium (as confirmed by CD spectra, Figure 3, B). These decreases are substantially less pronounced for catalysis with **1d**. Indeed, the CD spectra in all three conditions show a G-4 parallel signature (Figure 3, B).

Table 2. influence of counter ions on efficiency on sulfoxidation of 2-bromothioanisole. [a], [b]

G-4	Counter ion	Yield %	*e.e.* %
d($^{5'}$AGG GTT T$^{3'}$)]$_4$	K^+	6	61
	Na^+	3	1
	Li^+	2	-6
	K^+	9	65
1d	Na^+	9	56
	Li^+	3	52

[a] Conditions: [2-bromoanisole] = 5 mM; [H_2O_2] = 7.5 mM, [G-4] = 50 µM, [Cu(dmbipy)] = 50 µM, MOPS buffer 20 mM, pH 7.0, [XCl] = 150 mM, 15°C, 15 h. [b] Relative errors below 20 % on yields and *e.e.* were determined by statistical comparison of at least 5 experiments.

Another advantage of the increased stability of mimics was assessed. Indeed, in order to improve yields, quantities of the copper complex were increased using 1 % of either d($^{5'}$AGG GTT T$^{3'}$)]$_4$ or **1d** (Figure 6).

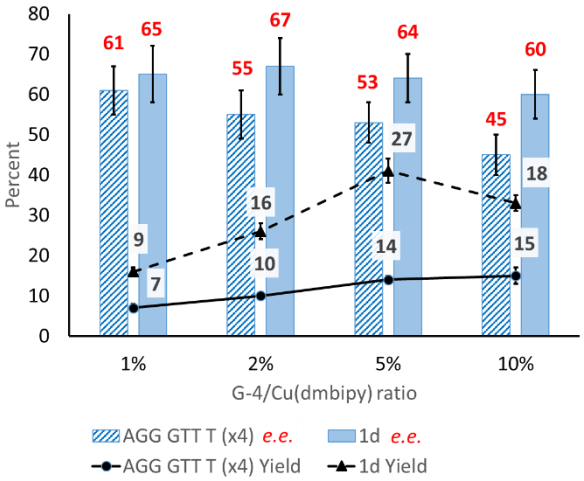

Figure 6. Influence of the quantity of Cu(dmbipy) on catalysis.

When more copper complex was introduced to the catalysis with tetramolecular G-4, the e.e. decreased while the yields increased slightly. This pattern, however, was not seen with **1d**. It implies that the tetramolecular G-4 is destabilized and that some racemic reaction takes place outside of its influence region. Increasing the quantity of copper most likely causes the oxidation of guanines into 8-oxo-guanines,[54] which leads to the instability of the tetramolecular G-4. Concerning **1d**, a slight decrease in *e.e*. is observed simultaneously with an increase in yield (reaching a maximum at 5 % copper), implying that the mimic's higher stability or rigidity either protects guanines from oxidation or allows the overall structure to be maintained despite the formation of 8-oxo-guanines.

SULFOXIDATION WITH THE ANTIPARALLEL MIMIC

Finally, the catalytic efficacy of mimic **2** was investigated for the asymmetric sulfoxidation of *p*-methylthioanisole and 2-bromothioanisole. Low yields (3 and 4 %, respectively) and no *e.e*. were obtained, whereas HT21 yielded 45 and 10 % with *e.e.* of 21 % and -46 %, respectively (Table 1). This observation is consistent with that of Can Li group[38] because, in the case of mimic **2**, the RAFT crowds the two areas of substrate interaction with the G-4 identified (Figure 1), demonstrating that asymmetric induction occurs where the contact is stronger.[38]

Conclusion

We have shown that constrained G-4 structures can help us comprehend G-4 enantioselective sulfoxidation. Our findings imply that, for parallel G-4, the reaction can take place at any of the three available reaction sites (the two outer tetrads and the grooves), and that different enantiomers can be formed depending on which site the reaction takes place preferentially/the quickest. If the reaction produces a racemic mixture, this can be due to either no interaction between the substrate and the G-4/Cu(dmbipy) complex or to antagonists' enantiomeric inductions at separate G-4 sites. As a result, by adding nucleosides, the reactivity can be controlled.
Furthermore, the structural stability provided by restricting the G-4 allows for greater flexibility in adjusting the reaction conditions as well as improved chemical stability of the structure under harsh conditions.

One disadvantage of using G-4 for sulfoxidation is that the reaction is substrate-dependent. This constraint, however, can be circumvented by modifying the G-4 topology depending on the substrate. For example, if the parallel G-4 cannot accomplish the asymmetric sulfoxidation of *p*-methylthioanisole, the antiparallel G-4 could.

Our findings for antiparallel and, by extension, hybrid native G-4 corroborate that the reaction occurs at the 3'-tetrad and/or the L2 loop in the case of HT21.[38]

Finally, since the reaction can occur at different sites and topologies, constrained G-4 provides a versatile platform for asymmetric sulfoxidation as well as hints about how the process works.

Experimental Section

SYNTHESES OF MIMICS

General

All solvents and reagents used were of the highest purity available. Protected Amino acids were obtained from Activotec and Novabiochem. Solvents and reactants were obtained from Aldrich, Novabiochem and Acros. Peptides **4,6** and Oligonucleotides **3a-h** and **5** were prepared adapting protocols previously described.[43,44] For peptides, reactions were monitored using UPLC-MS system Waters, with reverse phase chromatography using Nucleosil C18 column (130 Å, 2.1 x 50 mm, 1.7 µm) and detection by UV at 214 nm and 250 nm and by electron spray ionization mass spectrometry. A 0.6 mL/min flow linear gradient from 95 % solvent A (0.1 % formic acid in water) and 5 % solvent B (0.1% formic acid in acetonitrile) to 100 % B for 4 minutes was applied. RP HPLC purifications were performed on a Gilson or Waters system with Nucleosil C18 column (100 Å, 250 x 21 mm, 7 µm) with UV monitoring at 214 nm and 250 nm. A 22 mL/min flow linear gradient was applied from 95 % solvent A (0.1 % formic acid in water) and 5 % solvent B (0.1 % formic acid in acetonitrile) to 100 % B for 15 minutes.

For oligonucleotides and mimics **1a-h** and **2,** RP-UPLC-MS analysis were performed on a Waters UPLC-MS system, it includes reverse phase chromatography using Nucleosil C18 column (130 Å, 2.1 x 50 mm, 1.7 µm) and detection by UV at 260 nm and 280 nm and by electron spray ionization mass spectrometry. A 0.3 mL/min flow linear gradient was applied. Solvent C (triethylamine (15 mM) and hexafluoro-2-propanol (50 mM) in water) and solvent D (triethylamine (15 mM) and hexafluoro-2-propanol (50 mM) in methanol) were used.

Several gradients have been used: gradient I (0-30 % B in 12.5 minutes), gradient II (0-50 % B in 12.5 minutes). The RP-HPLC purifications of oligonucleotides were performed on a Gilson system with Nucleosil C-18 colunm (Macherey-Nagel, 100 Å, 250 x 10 mm, 7 µm) using 4 mL/min with UV monitoring at 260 nm and 280 nm. Solvent A (50 mM triethylammonium acetate buffer with 5% acetonitrile) and solvent B (acetonitrile with 5% water) were used. Desalting of oligonucleotides and mimics were performed by SEC on NAP 25 cartridge using the recommended protocol and quantifications of oligonucleotides was performed at 260 nm Molar extinction ε_{260nm} were estimated according to the nearest neighbor model.

General procedure for CuAAC.

To a solution of alkyne oligonucleotide (1.2 equiv., concentration 10^{-3} M) and azide peptide (1 equiv.) in 100 mM HEPES buffer (pH 7.4) were added $CuSO_4$ (2 equiv./ function), THPTA (20 equiv./ function) and sodium ascorbate (40 equiv./function). The reaction was stirred at room temperature for 2 h and quenched with a 0.5 M EDTA solution (50 equiv.). The product was purified on RP-HPLC then freeze-dried.

General procedure for oxime ligation

Aldehyde oligonucleotide (1 to 1.5 equiv. by oxyamine function) was dissolved in 0.4 M ammonium acetate buffer (pH 4.5, concentration 10^{-3} M) and free aminooxy peptide (1 equiv.) was added. The solution was stirred at room temperature for 2 h then the crude product was purified on RP-HPLC with a gradient from 0 % to 45 % solvent B in solvent A for 30 min.

Synthesis of mimic 1a

CuAAC ligation was carried out with alkyne containing oligonucleotide **3a** (4.4 equiv., 410 nmol) and peptide **4** (1 equiv., 93 nmol).The crude was purified on RP-HPLC and freeze-dried. (40 nmol, yield: 43 %, ε_{260nm} = 180 800 $M^{-1}.cm^{-1}$). Rt = 5.70 min (UPLC – gradient I). UPLC-ESI MS (-) m/z calcd for $C_{231}H_{309}N_{103}O_{106}P_{16}$: 6716.8; m/z found: 6716.0 $[M-H]^-$

Synthesis of mimic 1b

The CuAAC ligation was carried out with alkyne containing oligonucleotide **3b** (4.2 equiv., 444 nmol) and RAFT **4** (1 equiv., 105 nmol. The crude was purified on RP-HPLC and freeze-dried. (57 nmol, yield: 59 %, ε_{260nm} = 306 000 $M^{-1}.cm^{-1}$). Rt = 6.32 min (UPLC – gradient I). ESI MS (-) m/z calcd for $C_{351}H_{461}N_{139}O_{182}P_{28}$: 10406.5; m/z found: 10404.6 $[M-H]^-$

Synthesis of mimic 1c

The CuAAC ligation was carried out with alkyne containing oligonucleotide **3c** (4.2 equiv., 320 nmol) and RAFT **4** (1 equiv., 76 nmol).The crude was purified on RP-HPLC and freeze-dried. (22 nmol, yield: 43 %, ε_{260nm} = 277 200 $M^{-1}.cm^{-1}$). Rt = 8.27 min (UPLC – gradient I) ESI MS(-) m/z calcd for $C_{347}H_{461}N_{131}O_{186}P_{28}$: 10304.3; m/z found: 10309.9 $[M-H]^-$.

Synthesis of mimic 1d

The CuAAC ligation was carried out with alkyne containing oligonucleotide **3d** (4.2 equiv., 450 nmol) and RAFT **4** (1 equiv., 107 nmol). The crude was purified on RP-HPLC and freeze-dried. (70 nmol, yield: 65 %, ε_{260nm} = 279 600 $M^{-1}.cm^{-1}$). Rt = 7.03 min (UPLC – gradient I). ESI MS (-) m/z calcd for $C_{351}H_{465}N_{127}O_{190}P_{28}$: 10370.4; m/z found: 10371.1 $[M-H]^-$.

~~space~~

Synthesis of mimic 1e

The CuAAC ligation was carried out with alkyne containing oligonucleotide **3e** (4.2 equiv., 432 nmol) and RAFT **4** (1 equiv., 103 nmol). The crude was purified on RP-HPLC and freeze-dried. (32 nmol, yield: 31 %, ε_{260nm} = 214 800 $M^{-1}.cm^{-1}$). Rt = 8.10 min (UPLC – gradient I). MS-ESI (-) m/z calcd for $C_{271}H_{361}N_{111}O_{134}P_{20}$: 7932.9; m/z found: 7932.9 $[M-H]^-$.

Synthesis of mimic 1f

The CuAAC ligation was carried out with alkyne containing oligonucleotide **3f** (4.2 equiv., 327 nmol) and RAFT **4** (1 equiv., 78 nmol). The crude was purified on RP-HPLC and freeze-dried. (31 nmol, yield: 40 %, ε_{260nm} = 247 200 $M^{-1}.cm^{-1}$). Rt = 8.07 min (UPLC – gradient I). MS-ESI (-) m/z calcd for $C_{311}H_{413}N_{119}O_{162}P_{24}$: 9149.1; m/z found: 9149.1 $[M-H]^-$.

Synthesis of mimic 1g

The CuAAC ligation was carried out with alkyne containing oligonucleotide **3g** (4.2 equiv., 544 nmol) and RAFT **4** (1 equiv., 130 nmol).The crude was purified on RP-HPLC and freeze-dried. (44 nmol, yield: 34 %, ε_{260nm} = 312 000 $M^{-1}.cm^{-1}$). Rt = 8.27 min (UPLC – gradient I). MS-ESI/LTQ m/z calcd for $C_{391}H_{517}N_{135}O_{218}P_{32}$: 11581.5; m/z found: 11581.5 $[M-H]^-$.

Synthesis of mimic 1h

The CuAAC ligation was carried out with alkyne containing oligonucleotide **3h** (4.2 equiv., 402 nmol) and RAFT **4** (1 equiv., 96 nmol). The crude was purified on RP-HPLC and freeze-dried. (27 nmol, yield: 28 %, ε_{260nm} = 312 000 $M^{-1}.cm^{-1}$). Rt = 8.37 min (UPLC – gradient I). ESI MS (-) m/z calcd for $C_{471}H_{621}N_{151}O_{274}P_{40}$: 14020.7 m/z found: 14020.0 $[M-H]^-$.

Synthesis of mimic 7

First, the RAFT **6** was deprotected in a TFA/triisopropylsilane/H_2O (95/4.5/0.5, *v/v/v*) solution and the mixture was stirred for 30 min at room temperature. The solvent was then evaporated under vacuum and the crude peptide was precipitated in diethyl ether as a white powder~~s~~. The deprotection was considered as quantitative. Then oxime ligation was carried out with aldehyde containing oligonucleotide **5** (2.2 equiv., 580 nmol) and the deprotected RAFT (1 equiv., 260 nmol). The crude was purified on RP-HPLC and freeze-dried. (75 nmol, yield: 29 %, ε~~260nm~~ = 229 600 $M^{-1}.cm^{-1}$). Rt = 6.60 min (UPLC – gradient I); ESI MS (-) m/z calcd for $C_{287}H_{381}N_{113}O_{156}P_{24}$: 8648.9; m/z found: 8647.0 $[M-H]^-$.

Synthesis of mimic 2

The CuAAC ligation was carried out with the intermediate antiparallel conjugate **7** (1 equiv., 33 nmol). The crude was purified on RP-HPLC and freeze-dried. (20 nmol, yield: 60 %, ε_{260nm} = 229 000 $M^{-1}.cm^{-1}$). Rt = 5.02 min (UPLC – gradient I); ESI MS (-) m/z calcd for $C_{287}H_{381}N_{113}O_{156}P_{24}$: 8648.9 m/z found: 8647.0 $[M-H]^-$.

CATALYSIS EXPERIMENTS

General

All the reaction of sulfoxidation were thermostated at 15 °C and agitated by using a Thermomixer C (Eppendorf).

RP-UPLC-MS analysis were performed on a FLEXAR HPLC system, it includes reverse phase chromatography using a CHIRALAK® IG-3 column (2.1 x 150 mm, 3 µm) and detection by UV at 230 nm and 275 nm. A 0.2 mL/min flow was applied with solvent A (Water) and solvent B (acetonitrile). Several gradients have been used: gradient I (100 % B in 10 minutes), gradient II (95 % B in 10 minutes). All products and substrates were quantified and characterized by using calibration curves of the corresponding commercially available compounds.

Typical procedure for sulfoxidation reaction

G-4 (10 µM, unless otherwise stated) was added to a 3-(*N*-morpholino)propanesulfonic acid (MOPS) buffer (100 µL, 20 mM, pH 7.0) containing KCl (150 mM), heated for 3 min at 98 °C and annealed slowly over the course of 2 h to room temperature. Then, an aqueous solution of copper 4,4'-dimethyl-2,2'-bipyridine complex (50 µM) was added. The mixture was stirred for 0.5 h at 15 °C. Then, the sulfide dissolved in acetonitrile (1 µL of a 0.5 M solution, unless otherwise stated) was added. The reaction was started with the addition of H_2O_2 (7.5 µL of a 0.3 % aqueous solution). The reaction mixture was stirred for another 5 h at 15 °C. Then ethyl acetate (30 µL x 3) was added to extract the products and remained substrate. The extracted organic phase was diluted with acetonitrile (90 µL) and the crude product was directly analysed by chiral HPLC.

Calculation of the response factor for the references

The absorbance areas of sulfides and sulfoxides were measured at 275 nm and 230 nm, respectively. Each measurement was repeated at least 3 times. Quantities were estimated using calibration curves obtained with solution of commercially available thioethers and sulfoxides.

Supporting information

Protocols for synthesis of peptides and oligonucleotides and their characterization (UPLC, MS) as well as those of mimics. CD spectra of mimics **1a-h** and tetramolecular G-4. Denaturation experiments for **1d**, **1e** and **1h** and their corresponding native tetramolecular G-4 as well as those for **2.** Chromatograms resulting from catalysis experiments.

Acknowledgements

This work was supported by the French “Agence Nationale de la Recherche” (ANR-18-CE07-0017-01). LabEx “Arcane” (ANR-11-LABX-0003-01), CBH-EUR-GS (ANR-17-EURE-0003) and NanoBio-ICMG platforms (UAR 2607) are acknowledged for their support.

Keywords: Asymmetric Sulfoxidation. Nucleic acids, G-quadruplexes, Constrained G-4.

References

[1] C. A. Busacca, D. R. Fandrick, J. J. Song, C. H. Senanayake, *Adv. Synth. Catal.* **2011**, *353*, 1825–1864.
[2] B. M. Nestl, S. C. Hammer, B. A. Nebel, B. Hauer, *Angew. Chem. Int. Ed.* **2014**, *53*, 3070–3095.
[3] J. Bos, G. Roelfes, *Curr. Opin. Chem. Biol.* **2014**, *19*, 135–143.
[4] H. J. Davis, T. R. Ward, *ACS Cent. Sci.* **2019**, *5*, 1120–1136.
[5] Gerard Roelfes, F. Feringa, *Angewandte Chemie* **2005**, *117*, 3294–3296.
[6] D. Coquière, B. L. Feringa, G. Roelfes, *Angew. Chem. Int. Ed.* **2007**, *46*, 9308–9311.
[7] A. J. Boersma, J. E. Klijn, B. L. Feringa, G. Roelfes, *J. Am. Chem. Soc.* **2008**, *130*, 11783–11790.
[8] N. Shibata, H. Yasui, S. Nakamura, T. Toru, *Synlett* **2007**, *2007*, 1153–1157.
[9] E. W. Dijk, A. J. Boersma, B. L. Feringa, G. Roelfes, *Org. Biomol. Chem.* **2010**, *8*, 3868–3873.
[10] P. Fournier, R. Fiammengo, A. Jäschke, *Angew. Chem. Int. Ed.* **2009**, *48*, 4426–4429.
[11] Ana Rioz-Martínez, Jens Oelerich, Nathalie Ségaud, G. Roelfes, *Angewandte Chemie* **n.d.**, DOI 10.1002/ange.201608121.
[12] S. Dey, C. L. Rühl, A. Jäschke, *Chem. Eur. J.* **2017**, *23*, 12162–12170.
[13] J. H. Yum, H. Sugiyama, S. Park, *The Chemical Record* **2022**, *22*, e202100333.
[14] I. Willner, B. Shlyahovsky, M. Zayats, B. Willner, *Chem. Soc. Rev.* **2008**, *37*, 1153–1165.
[15] J. Kosman, B. Juskowiak, *Anal. Chim. Acta* **2011**, *707*, 7–17.
[16] P. Travascio, Y. Li, D. Sen, *Chem. Biol.* **1998**, *5*, 505–517.
[17] E. Golub, R. Freeman, I. Willner, *Angew. Chem. Int. Ed.* **2011**, *50*, 11710–11714.
[18] Y. Guo, J. Chen, M. Cheng, D. Monchaud, J. Zhou, H. Ju, *Angew. Chem. Int. Ed.* **2017**, *56*, 16636–16640.
[19] L. C. H. Poon, S. P. Methot, W. Morabi-Pazooki, F. Pio, A. J. Bennet, D. Sen, *J. Am. Chem. Soc.* **2011**, *133*, 1877–1884.
[20] J. Hao, W. Miao, Y. Cheng, S. Lu, G. Jia, C. Li, *ACS Catal.* **2020**, *10*, 6561–6567.
[21] J. Hao, W. Miao, S. Lu, Y. Cheng, G. Jia, C. Li, *Chem. Sci.* **2021**, *12*, 7918–7923.
[22] S. Roe, D. J. Ritson, T. Garner, M. Searle, J. E. Moses, *Chem. Commun.* **2010**, *46*, 4309–4311.
[23] C. Wang, G. Jia, J. Zhou, Y. Li, Y. Liu, S. Lu, C. Li, *Angew. Chem. Int. Ed.* **2012**, *51*, 9352–9355.
[24] M. P. Cheng, J. Zhou, G. Q. Jia, X. J. Ai, J. L. Mergny, C. Li, *Biochim. Biophys. Acta-Gen. Subj.* **2017**, *1861*, 1913–1920.
[25] C. Wang, Y. Li, G. Jia, Y. Liu, S. Lu, C. Li, *Chem. Commun.* **2012**, *48*, 6232–6234.
[26] K. Chen, Z. He, W. Xiong, C.-J. Wang, X. Zhou, *Chinese Chemical Letters* **2021**, *32*, 1701–1704.
[27] P. M. Punt, M. D. Langenberg, O. Altan, G. H. Clever, *J. Am. Chem. Soc.* **2021**, *143*, 3555–3561.
[28] J. H. Yum, S. Park, H. Sugiyama, *Org. Biomol. Chem.* **2019**, *17*, 9547–9561.
[29] M. Cheng, Y. Li, J. Zhou, G. Jia, S.-M. Lu, Y. Yang, C. Li, *Chem. Commun.* **2016**, *52*, 9644–9647.
[30] C. Festa, V. Esposito, D. Benigno, S. De Marino, A. Zampella, A. Virgilio, A. Galeone, *International Journal of Molecular Sciences* **2022**, *23*, DOI 10.3390/ijms23031092.
[31] E. Wojaczyńska, J. Wojaczyński, *Chem. Rev.* **2020**, *120*, 4578–4611.
[32] Y. Ma, K. Iida, K. Nagasawa, *Biochemical and Biophysical Research Communications* **2020**, *531*, 3–17.
[33] S. Burge, G. N. Parkinson, P. Hazel, A. K. Todd, S. Neidle, *Nucleic Acids Res.* **2006**, *34*, 5402–5415.
[34] A. T. Phan, V. Kuryavyi, D. J. Patel, *Current Opinion in Structural Biology* **2006**, *16*, 288–298.
[35] J. T. Davis, *Angew. Chem. Int. Ed. Engl.* **2004**, *43*, 668–98.
[36] M. Bončina, G. Vesnaver, J. B. Chaires, J. Lah, *Angewandte Chemie International Edition* **2016**, *55*, 10340–10344.
[37] E. Largy, J.-L. Mergny, V. Gabelica, in *The Alkali Metal Ions: Their Role for Life* (Eds.: A. Sigel, H. Sigel, R.K.O. Sigel), Springer International Publishing, Cham, **2016**, pp. 203–258.
[38] Y. Cheng, M. Cheng, J. Hao, G. Jia, C. Li, *ChemBioChem* **2018**, *19*, 2233–2240.
[39] D. Monchaud, M. P. Teulade-Fichou, *Org. Biomol. Chem.* **2008**, *6*, 627–636.
[40] B. Heddi, A. T. Phan, *J. Am. Chem. Soc.* **2011**, *133*, 9824–9833.
[41] Y. Wang, D. Patel, *Structure* **1993**, *1*, 263–282.
[42] E. Gavathiotis, M. S. Searle, *Org. Biomol. Chem.* **2003**, *1*, 1650–1656.

[43] P. Murat, D. Cressend, N. Spinelli, A. Van der Heyden, P. Labbe, P. Dumy, E. Defrancq, *ChemBioChem* **2008**, *9*, 2588–2591.
[44] R. Bonnet, T. Lavergne, B. Gennaro, N. Spinelli, E. Defrancq, *Chem. Commun.* **2015**, *51*, 4850–3.
[45] R. del Villar-Guerra, J. O. Trent, J. B. Chaires, *Angewandte Chemie International Edition* **2018**, *57*, 7171–7175.
[46] M. Vorlíčková, I. Kejnovská, J. Sagi, D. Renčiuk, K. Bednářová, J. Motlová, J. Kypr, *Methods* **2012**, *57*, 64–75.
[47] C. C. Hardin, T. Watson, M. Corregan, C. Bailey, *Biochemistry* **1992**, *31*, 833–841.
[48] J. L. Mergny, A. De Cian, A. Ghelab, B. Sacca, L. Lacroix, *Nucleic Acids Res.* **2005**, *33*, 81–94.
[49] C. Cáceres, G. Wright, C. Gouyette, G. Parkinson, J. A. Subirana, *Nucleic Acids Research* **2004**, *32*, 1097–1102.
[50] S. M. Haider, S. Neidle, G. N. Parkinson, *Biochimie* **2011**, *93*, 1239–1251.
[51] W. Li, Y. Li, Z. L. Liu, B. Lin, H. B. Yi, F. Xu, Z. Nie, S. Z. Yao, *Nucleic Acids Res.* **2016**, *44*, 7373–7384.
[52] A. Draksharapu, A. J. Boersma, M. Leising, A. Meetsma, W. R. Browne, G. Roelfes, *Dalton Transactions* **2015**, *44*, 3647–3655.
[53] A. Draksharapu, A. J. Boersma, W. R. Browne, G. Roelfes, *Dalton Transactions* **2015**, *44*, 3656–3663.
[54] L. J. Kennedy, K. Moore, J. L. Caulfield, S. R. Tannenbaum, P. C. Dedon, *Chem. Res. Toxicol.* **1997**, *10*, 386–392.

Entry for the Table of Contents

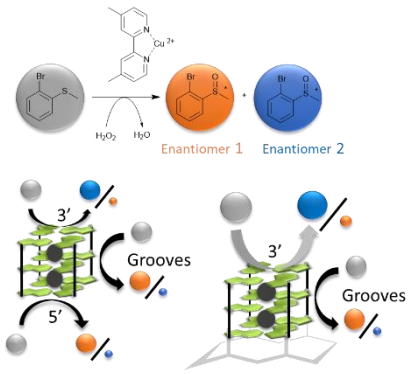

G-quadruplexes (G-4) mediated asymmetric sulfoxidation. Asymmetric sulfoxidations were performed utilizing native or modified G-4-forming nucleic acids as chiral inductors, providing proof that asymmetric reactions can occur at distinct sites of the biomolecule, yielding different enantiomers.